Efficient electrolyte of *N*,*N*′-bis(salicylidene)ethylenediamine zinc(II) iodide in dye-sensitized solar cells

Shuming Yang,*[a] Huizhi Kou,[a] Hongjun Wang,[a] Ke Cheng[b] and Jichao Wang[a]

Received (in Victoria, Australia) 30th June 2009, Accepted 26th October 2009
First published as an Advance Article on the web 8th December 2009
DOI: 10.1039/b9nj00405j

N,*N*′-Bis(salicylidene)ethylenediamine zinc(II) iodide ($ZnLI_2$) was synthesized and characterized by elemental analysis, UV-Vis and IR spectroscopies. This new Schiff base complex was, for the first time, applied as the electrolyte of a dye-sensitized solar cell. $ZnLI_2$ has high reductive activity and conductivity, resulting in larger IPCE and photoelectric conversion efficiency in the DSSCs. The best results were obtained in the optimized composite electrolyte E2, with a photoelectric conversion efficiency of 7.75% under 100 mW cm^{-2} irradiation. This work provides a new approach for the improvement of the photoelectrochemical properties of dye-sensitized solar cells.

Introduction

Dye-sensitized solar cells (DSSCs), also known as Grätzel cells, are photovoltaic devices with promising applications in the production of clean and sustainably produced energy.[1–4] A unique feature of these solar cells is the nanoporous electrode formed by nanocrystalline semiconductor. The nanoporous electrode is sensitized with dye molecules and embedded in an electrolyte solution that contains a redox couple, such as I^-/I_3^-. The nanoporous electrode is critical, because it has a large surface area to anchor dye molecules in which electrons can be excited and injected into the nanoporous semiconductor film. The electrolyte also plays a very important role, because it must regenerated the oxidized dye molecules. Therefore much effort has been put into the development of efficient electrolytes to achieve high cell performance. So far, several kinds of electrolytes have been used in DSSCs, including liquid electrolytes,[5,6] quasi-solid electrolytes[7,8] and solid electrolytes.[9–11] The latter two do decrease the risk associated with leakage of liquid electrolytes, but the photoelectric conversion efficiencies of the cells fabricated from them are not satisfactory, mainly due to the low ionic conductivity of the electrolytes and/or poor electrode–electrolyte contact. The highest photoelectric conversion efficiency was achieved in DSSCs with liquid electrolytes containing I_3^-/I^- the redox couple.[12] In research into liquid electrolytes, it has been demonstrated that cations play an important role in achieving high conversion efficiencies. For example, the multilayer adsorption of imidazolium cations as the counterion of I^- and I_3^- leads to an increase of the electron diffusion coefficient with increasing cation concentration, which dramatically improves DSSC performance.[13–15]

It has been reported that small metal ions, such as Li^+ ions, can be adsorbed and inserted into TiO_2 nanoporous films.[16–20] On one hand, a cation adsorbed on a surface generates an increase of electrical potential in the Helmholtz layer[21] in such way that it favors electron injection from the dye LUMO towards the TiO_2 conduction band, and recombination will be diminished because the adsorbed cations will shield electron back-flow through the TiO_2 surface; therefore there will be an increase in the photocurrent generated by the solar cell, but V_{oc} will drop.[22] On the other hand, metal ions inserted into TiO_2 lattices will combine with electrons in the conduction band to form a dipole (such as Li^+–e^-), which facilitates recombination between the dipole Li^+–e^- and I_3^- in the electrolyte.[16–19] Zn^{2+} can be also inserted into the TiO_2 lattices to some extent, because the sizes of Zn^{2+} and Li^+ ions are comparable (R = 0.074 and 0.068 nm, respectively).[20] Our purpose is to apply metal complex iodide to minimize the negative effects of the insertion of small metal ions into TiO_2 lattices in order to improve the photoelectrochemical properties of TiO_2 nanoporous electrodes. Electrolytes containing Schiff base cations in DSSCs have not been reported so far. In this study a new Schiff base iodide complex (*N*,*N*′-bis(salicylidene)ethylenediamine zinc(II) iodide) was synthesized and applied as a DSSC electrolyte.

Experimental section

Materials and solutions

Optically transparent electrodes (OTEs) were made from an F-doped SnO_2-coated glass plate. Water (R = 18 MΩ) from an Easypure RF system was used in the preparation of all solutions. $Ti(OiPr)_4$, *tert*-butylpyridine and ethyl cellulose were purchased from Acros. Salicylidene, ethylenediamine, 1-chloropropane, terpineol, *N*-methylimidazole, zinc iodide and propionitrile purchased from the Beijing Reagent Co., were reagent grade, while propionitrile was distilled over P_2O_5 before use. The dye N3 was synthesized according to the literature.[23] 1-Methyl-3-propylimidazolium iodide (PMII) was synthesized according to the literature.[24]

[a] *College of Chemistry and Chemical Engineering, Institute of Applied Chemistry, Xinyang Normal University, Henan, 464000, China. E-mail: smyang2006@163.com; Tel: +86-0376-6393736*
[b] *Key Laboratory of Special Functional Materials, Henan University, Kaifeng, Henan, 475001, China*

Instrumentation

The absorption spectra of L and $ZnLI_2$ were recorded on an UV-1240 spectrophotometer (Shimadzu, Japan). The infrared spectra of the chemicals, in KBr disks, were determined with a Tensor 27 spectrometer in the 4000–400 cm^{-1} region. CHN analyses were obtained using a 240C elemental analysis instrument (Perkin-Elmer). ^1H and ^{13}C NMR spectra were recorded on a Bruker 400 spectrometer in acetone-d_6 with TMS as internal standard. Electrochemical and photoelectrochemical experiments were performed on a CH800 electrochemical analyzer (CH Instrument). A 500 W xenon lamp was used as the source of excitation. A KG4 filter (Schott) was set in the light beam to protect the electrodes from heating, and a GG420 cutoff filter (Schott) was used to prevent the TiO_2 film from being excited by light with wavelength less than 400 nm. To achieve a given band-pass of light, the light beam was passed through a group of filters (Ealing Co.). The effective illumination area of a flat window was 0.196 cm^2. Ionic conductivity measurements of electrolytes were conducted on a CDM210 conductivity meter (Radiometer Analytical, SAS, France).

Synthesis of *N*,*N*′-bis(salicylidene)ethylenediamine (denoted as L)

N,*N*′-Bis(salicylidene)ethylenediamine was synthesized following the published procedure with a small modification.[25] The route is shown in Scheme 1.

10.0 g salicylaldehyde was dissolved in 45 ml ethanol and heated to 40 °C, and then added dropwise to a solution of 2.4 g ethylenediamine in ethanol under vigorous stirring. The mixture solution turned light yellow, and for a while yellow sheet-like crystals precipitated out. After 20 min, the mixture was cooled and the precipitate collected. The yellow solid was re-crystallized in ethanol and dried at room temperature under vacuum. Anal. Calc. for $C_{16}H_{16}N_2O_2$ (F.W.: 268.31): C, 71.62; H, 6.01; N, 10.44%. Found: C, 71.48; H, 5.96; N, 10.45%.

Synthesis of *N*,*N*′-Bis(salicylidene)ethylenediamine zinc(II) iodide (denoted as $ZnLI_2$)

The synthesis route of $ZnLI_2$ shown in Scheme 2.

All operations were carried out under an argon atmosphere. 1.5 g of ligand L was dissolved in 125 mL of dry methanol. To this solution was added 1.75 g ZnI_2 methanol solution under stirring. After completion of addition the mixture solution was stirred and refluxed for 3 h, and the methanol evaporated under vacuum. The solid obtained was washed with CH_2Cl_2, filtered, and the product collected and dried at room temperature under vacuum. Anal. Calc. for $ZnC_{16}H_{16}N_2O_2I_2$ (F.W.: 587.51): C, 32.71; H, 2.75; N, 4.77%. Found: C, 32.62; H, 2.70; N, 4.79%.

Preparation of the dye-sensitized nanoporous electrodes

The preparation of the nanocrystalline TiO_2 paste and its films on conductive glass was similar to that previously reported.[26] Generally, a TiO_2 suspension was spread on the substrates using a glass rod with adhesive tapes as spacers. The films were dried at 125 °C and sintered at 450 °C for 30 min in air.

For sensitization with the dye, the TiO_2 film was immersed in 5×10^{-4} mol L^{-1} N3 absolute ethanol solution for 12 h at room temperature. To minimize adsorption of moisture from the air, the electrodes were dipped in the dye solution while they were still warm (80 °C). The dye-sensitized electrodes were then rinsed thoroughly with ethanol and dried.

Results and discussion

Absorption spectra

The absorption spectra of the ligand (L) and complex ($ZnLI_2$) in absolute methanol were measured. The spectra are shown in Fig. 1.

The absorption spectrum of ligand L in methanol shows three broad bands at 255, 315 and 408 nm, which are assigned to the intraligand $\pi \rightarrow \pi^*$ and $n \rightarrow \pi^*$ transitions, respectively.[27] There is no d–d transition in the complex due to Zn(II), which has a d^{10} electronic structure. In contrast to L, the absorption peak at 408 nm of the complex ($ZnLI_2$) disappears due to the coordination of the non-bonded electron pairs of the N atom with Zn(II). The shorter wavelength band of the complex ($ZnLI_2$) is 5 nm red-shifted from 315 nm to 320 nm. The red-shift mainly results from the coordination of ligand with Zn(II), which weakens the conjugation plane of the complex and lowers the energy of the π^* orbital of the ligand, causing the $\pi \rightarrow \pi^*$ transition to occur at lower energy.

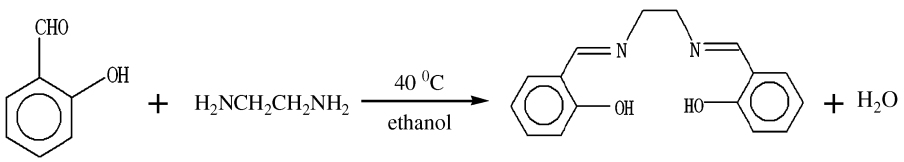

Scheme 1 Synthetic route to *N*,*N*′-bis(salicylidene)ethylenediamine.

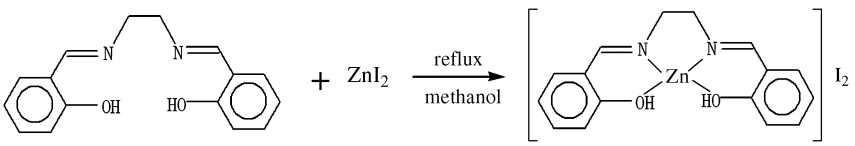

Scheme 2 Synthetic route to *N*,*N*′-bis(salicylidene)ethylenediamine zinc(II) iodide.

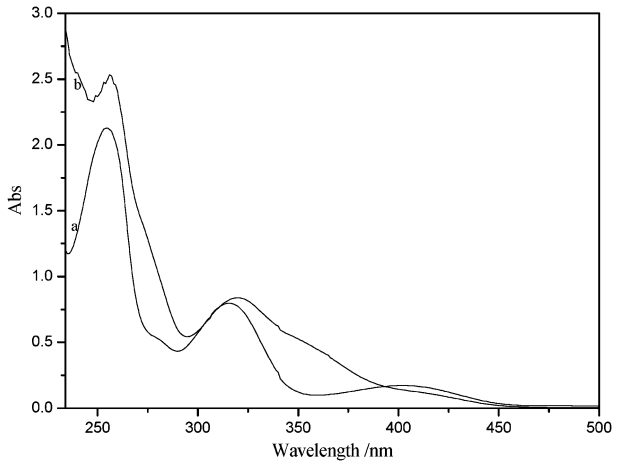

Fig. 1 UV-vis absorption spectra of L and $ZnLI_2$ in 1.0×10^{-4} mol L^{-1} methanol solutions: (a) L; (b) $ZnLI_2$.

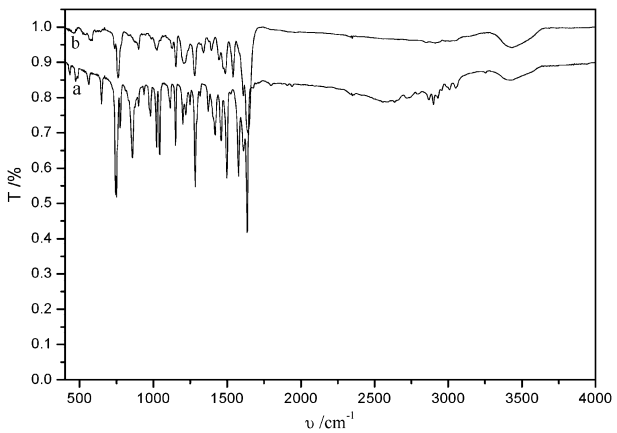

Fig. 2 IR spectra of L and $ZnLI_2$ in the range 4000–400 cm^{-1}: (a) L; (b) $ZnLI_2$.

Infrared spectra

Spectra of the solids in KBr disks were measured in the 4000–400 cm^{-1} region (Fig. 2). The main vibration data are listed in Table 1.

The characteristic peaks of the Schiff base ligand and its zinc complex are in 1670–1500 cm^{-1} region. It has been found that the C=N stretching frequencies of a complex will increase by 5–10 cm^{-1} if a Schiff base ligand coordinates to the metal ion as a neutral molecule.[28] Our experiment showed that the C=N stretching vibration of the free ligand L was at 1635 cm^{-1}, while that of the Zn(II) complex was at 1642 cm^{-1}. The C=N stretching frequencies are shifted to higher frequencies by *ca.* 7 cm^{-1} upon complexation, indicating that the ligand coordinates to Zn(II) ion as a neutral molecule. Two aromatic C=C vibrations should occur in the 1577–1450 cm^{-1} region, and both bands will shift to lower frequencies upon coordination with metal ions.[29] For our synthesized ligand these two vibrations occur at 1577 and 1497 cm^{-1}, respectively, while that of the zinc complex occurs at 1540 and 1486 cm^{-1}, respectively. The two bands shift to lower frequency by 37 and 11 cm^{-1}, respectively. The Ar–O stretching frequency appears as a strong band in the 1263–1213 cm^{-1} region.[30] For the ligand L and the complex, the vibrations occur at 1284 cm^{-1} and 1281 cm^{-1}, respectively. The Ar–O stretching frequency is shifted by 3 cm^{-1} to lower frequency, indicating that a Zn(II)–O bond was formed.[29,31] It should be noted that there is a complex band in the region 3100–2800 cm^{-1} in the ligand which can be assigned to an intramolecular hydrogen bond.[32,33] However, this band almost disappears in the Zn complex, indicating that the intramolecular hydrogen bond becomes broken, which is most probably due to the coordination of Zn with N and O.

Table 1 IR data of ligand L and $ZnLI_2$

	IR band (cm^{-1})		
Substance	C=N	Ar–O	C=C
L	1635s	1284s	1577s, 1497s
$ZnLI_2$	1642s	1281s	1540s, 1486s

The structure of the Zn complex was further confirmed by its NMR spectra. The ^1H NMR spectrum clearly shows that there are four kinds of hydrogen atoms (δ, ppm): 3.94 (s, 2H, N–CH_2), 6.84–7.31 (m, 4H, Ph), 8.36 (m, 1H, N=CH), 13.24 (w, 1H, Ph–OH). The ^{13}C NMR spectrum shows that there are eight kinds of carbon atoms (δ, ppm): 118.6, 160.9, 116.9, 132.3, 118.6, 131.4, 166.4, 59.7.

Incident photon-to-current efficiency (IPCE)

The IPCE values of the DSSCs based on several electrolytes were plotted *vs.* wavelength, and are shown in Fig. 3.

The maximum IPCE increased from 49% to 68%, with the DSSC based on E2 having the highest value throughout the visible wavelengths. It is also seen that $ZnLI_2$ is quite efficient when it was applied as the sole redox species. In this study the composition of the electrolyte was optimized in order to obtain maximum photocurrent. It has been reported that increasing cation size tends to increase the reductive activity of I^- in DSSCs,[34] which could facilitate the reduction of

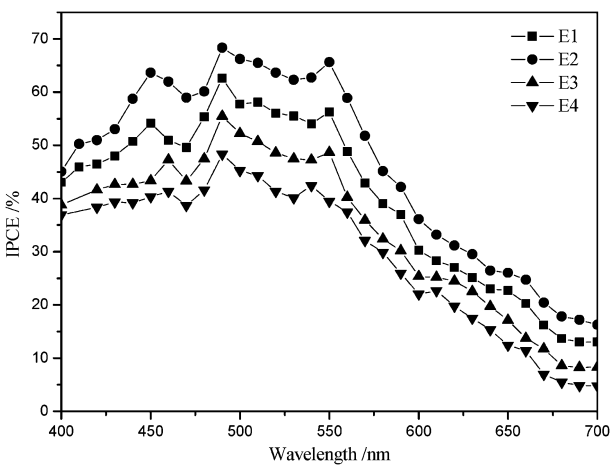

Fig. 3 IPCE curves of dye-sensitized TiO_2 electrodes. Electrolyte: E1: 0.1 mol L^{-1} ZnI_2, 0.05 mol L^{-1} I_2, 0.5 mol L^{-1} TBP and 0.6 mol L^{-1} PMII; E2: 0.1 mol L^{-1} $ZnLI_2$, 0.05 mol L^{-1} I_2, 0.5 mol L^{-1} TBP and 0.6 mol L^{-1} PMII; E3: 0.05 mol L^{-1} I_2, 0.5 mol L^{-1} TBP and 0.6 mol L^{-1} PMII; E4: 0.25 mol L^{-1} $ZnLI_2$, 0.05 mol L^{-1} I_2, 0.5 mol L^{-1} TBP. The solvent is propionitrile.

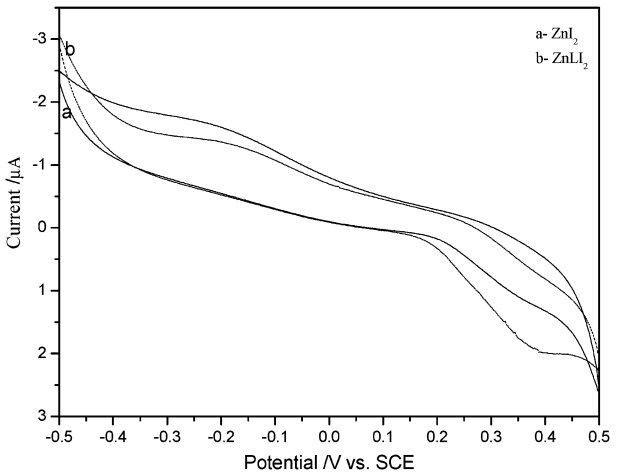

Fig. 4 Cyclic voltammograms of ZnI_2 and $ZnLI_2$ in 1.0×10^{-4} mol L^{-1} propionitrile solutions. The working and counter electrodes were platinum disks, and the reference was a saturated calomel electrode (SCE). The supporting electrolyte was 1 mol L^{-1} $LiClO_4$, and the scan rate was 10 mV s^{-1}.

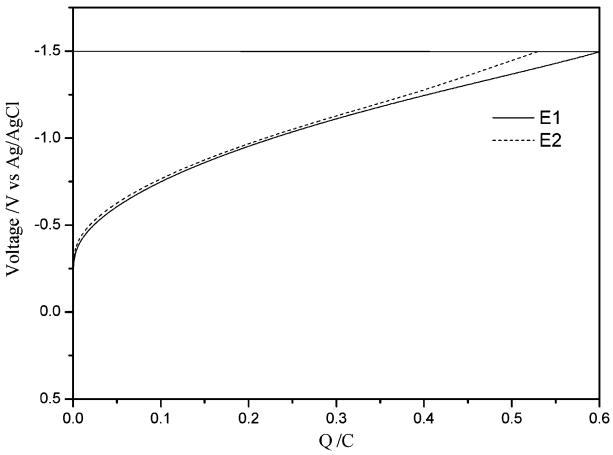

Fig. 5 Energy levels of TiO_2 electrodes in different electrolytes as a function of charge. Electrolyte: E1: 0.1 mol L^{-1} ZnI_2, 0.05 mol L^{-1} I_2, 0.5 mol L^{-1} TBP and 0.6 mol L^{-1} PMII; E2: 0.1 mol L^{-1} $ZnLI_2$, 0.05 mol L^{-1} I_2, 0.5 mol L^{-1} TBP and 0.6 mol L^{-1} PMII. The solvent is propionitrile.

oxidized dyes. In our case ZnL^{2+} is much bigger than Zn^{2+}, so a bigger photocurrent or IPCE was expected for $ZnLI_2$. In addition the cyclic voltammograms of ZnI_2 and $ZnLI_2$ were measured in propionitrile, and the results are shown in Fig. 4. It can be seen that the reductive activity of I^- in $ZnLI_2$ is higher than that in ZnI_2, which also could facilitate the reduction of oxidized dyes, resulting in higher J_{sc} or IPCE.

In order to investigate other reasons for the beneficial role of $ZnLI_2$, the ion conductivities of ZnI_2 and $ZnLI_2$ in propionitrile were measured, and the results are summarized in Table 2.

It is striking that the conductivities of $ZnLI_2$ are much higher than that of ZnI_2, whether on its own or with I_2 in propionitrile. The behavior is understandable because the complex ion of ZnL^{2+} should be more compatible with the organic solvent. Generally, higher ion conductivities should result in a bigger DSSC photocurrent,[35] in agreement with our photoelectrochemical measurements.

We then investigated whether there was any influence of the electrolyte on the band level of TiO_2. The voltage–current characteristics of TiO_2 electrodes based on each electrolyte were measured in a three-electrode system, and the results are shown in Fig. 5.

It can be seen that there are gradual onsets of charges due to the injection of the surface-trapped electrons below the conduction band edge.[36] The onset of the TiO_2 electrodes are almost the same in both electrolytes, implying that the electrolytes had little influence on the conduction band of TiO_2.

Table 2 Ionic conductivities (σ) of ZnI_2 and $ZnLI_2$ in propionitrile

Electrolyte (13 °C)	σ (S m^{-1})
ZnI_2 (0.1 mol L^{-1})	0.0461
$ZnLI_2$ (0.1 mol L^{-1})	0.1321
ZnI_2 (0.1 mol L^{-1}) + I_2 (0.05 mol L^{-1})	0.3480
$ZnLI_2$ (0.1 mol L^{-1}) + I_2 (0.05 mol L^{-1})	0.5230

The photoelectric conversion efficiency

For photoelectric conversion efficiency measurements, a thin sandwich-type solar cell was fabricated. An N3-sensitized TiO_2 electrode was used as the photoanode and a Pt-coated F-doped SnO_2 electrode as the photocathode. Fig. 6 presents the photocurrent–photovoltage curves measured for several electrolytes under 100 mW cm^{-2} white light irradiation.

The cell photoelectric parameters of the DSSCs based on several electrolytes are listed in Table 3. The best results were obtained with E2 as the electrolyte. It is particularly notable that the improved η mainly results from the increased J_{sc}. As discussed previously, the increased J_{sc} could result from the higher reductive activity and higher ion conductivities of

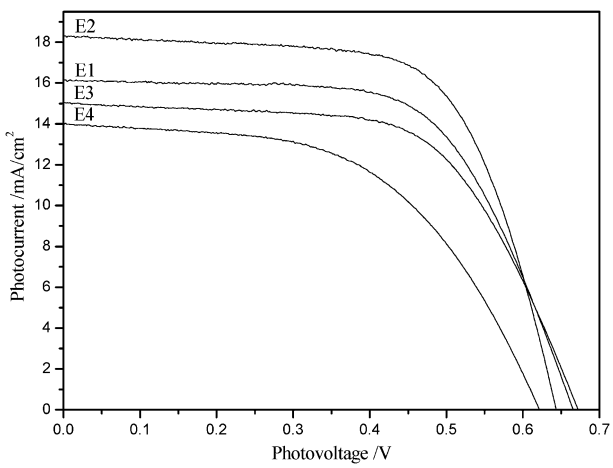

Fig. 6 Photocurrent–photovoltage curves of dye-sensitized TiO_2 electrodes based on different electrolytes. Electrolyte: E1: 0.1 mol L^{-1} ZnI_2, 0.05 mol L^{-1} I_2, 0.5 mol L^{-1} TBP and 0.6 mol L^{-1} PMII; E2: 0.1 mol L^{-1} $ZnLI_2$, 0.05 mol L^{-1} I_2, 0.5 mol L^{-1} TBP and 0.6 mol L^{-1} PMII; E3: 0.05 mol L^{-1} I_2, 0.5 mol L^{-1} TBP and 0.6 mol L^{-1} PMII; E4: 0.25 mol L^{-1} $ZnLI_2$, 0.05 mol L^{-1} I_2, 0.5 mol L^{-1} TBP. The solvent is propionitrile.

Table 3 The cell parameters of DSSCs based on different electrolytes

Electrolyte	J_{sc} (mA cm^{-2})	V_{oc} (V)	FF	η (%)
E1	16.16	0.66	0.64	6.77
E2	18.34	0.64	0.66	7.75
E3	15.05	0.67	0.61	6.19
E4	13.99	0.62	0.54	4.72

$ZnLI_2$, consistent with their IPCE behavior. On the other hand, because the conduction band edge was similar for the two electrolytes, the photovoltage was not expected to be much improved. Therefore, the improvement of the photoelectric conversion efficiency of the electrode based on E2 must primarily come from the improvement of the photocurrent, not from the photovoltage.

Conclusions

In summary, *N*,*N*′-bis(salicylidene)ethylenediamine zinc(II) iodide was synthesized and applied as an electrolyte in dye-sensitized solar cells. The higher reductive activity and higher conductivities of $ZnLI_2$ resulted in an increase in short-circuit photocurrent, IPCE and photoelectric conversion efficiency of the DSSC with E2. $ZnLI_2$ is quite efficient when it applied as the sole redox species of the DSSC. The best results were obtained with the optimized electrolyte E2, for which the short-circuit photocurrent density (J_{sc}), open-circuit photovoltage (V_{oc}), fill factor (FF) and the photoelectric conversion efficiency (η) were 18.34 mA cm^{-2}, 0.64 V, 0.66 and 7.75%, respectively. Our research showed that electrolytes such as $ZnLI_2$ could be promising in dye-sensitized solar cells.

Acknowledgements

This work was supported financially by the National Natural Science Foundation of China (Grant No. 20773103), the Scientific Research Foundation for the Returned Overseas Chinese Scholars, State Education Ministry (2008101), Selected Programs for Scholars back from Overseas, Ministry of Personnel (2006164) and the Science & Technology Program of the Education Department of Henan (2008A150022).

References

1 M. Grätzel, *Nature*, 2001, **414**, 338.
2 M. Grätzel, *J. Photochem. Photobiol., C*, 2003, **4**, 145.
3 M. Grätzel, *J. Photochem. Photobiol., A*, 2004, **164**, 3.
4 A. Hagfeldt and M. Grätzel, *Chem. Rev.*, 2000, **33**, 269.
5 P. Wang, S. M. Zakeeruddin, J. E. Moser and M. Grätzel, *J. Phys. Chem. B*, 2003, **107**, 13280.
6 M. K. Nazeeruddin, P. Péchy and T. J. Renouard, *J. Am. Chem. Soc.*, 2001, **123**, 1613.
7 A. F. Nogueda, J. R. Durrant and M. A. Depaoli, *Adv. Mater.*, 2001, **13**, 826.
8 O. A. Ileperuma, M. A. K. L. Dissanayake and S. Somasundaram, *Electrochim. Acta*, 2002, **47**, 2801.
9 Q. B. Meng, K. Takahashi, X. T. Zhang, I. Sutanto, T. N. Rao, O. Sato and A. Fujishima, *Langmuir*, 2003, **19**, 3572.
10 F. O. Lenzmann, B. C. O'Regan, J. J. T. Smits, H. P. C. E. Kuipers, P. M. Sommeling, L. H. Slooff and J. A. M. van Roosmalen, *Progr. Photovolt.: Res. Appl.*, 2005, **13**, 333.
11 G. P. Smestad, S. Spiekermann, J. Kowalik, C. D. Grant, A. M. Schwartzberg, J. Zhang, L. M. Tolbert and E. Moons, *Sol. Energy Mater. Sol. Cells*, 2003, **76**, 85.
12 M. Grätzel, *Inorg. Chem.*, 2005, **44**, 6841.
13 S. Kambe, S. Nakade, T. Kitamura, Y. Wada and S. Yanagida, *J. Phys. Chem. B*, 2002, **106**, 2967.
14 W. Kubo, S. Kambe, S. Nakade, T. Kitamura, K. Hanabusa, Y. Wada and S. Yanagida, *J. Phys. Chem. B*, 2003, **107**, 4374.
15 K. Hara, T. Horiguchi, T. Kinoshita, K. Sayama and H. Arakawa, *Sol. Energy Mater. Sol. Cells*, 2001, **70**, 151.
16 H. Lindstro1m, S. So1dergren, A. Solbrand, H. Rensmo, J. Hjelm, A. Hagfeldt and S. E. Lindquist, *J. Phys. Chem. B*, 1997, **101**, 7710.
17 H. Lindstrolm, S. Soldergren, A. Solbrand, H. Rensmo, J. Hjelm, A. Hagfeldt and S. E. Lindquist, *J. Phys. Chem. B*, 1997, **101**, 7717.
18 G. Boschloo and D. Fitzmaurice, *J. Electrochem. Soc.*, 2000, **147**, 1117.
19 G. Boschloo and D. Fitzmaurice, *J. Phys. Chem. B*, 1999, **103**, 2228.
20 J. W. Long, L. R. Qadir, R. M. Stroud and D. R. Rolison, *J. Phys. Chem. B*, 2001, **105**, 8712.
21 D. Cahen, G. Hodes, M. Grätzel, J. F. Guillemoles and I. Riess, *J. Phys. Chem. B*, 2000, **104**, 2053.
22 R. E. Ramırez and E. M. Sanchez, *Sol. Energy Mater. Sol. Cells*, 2006, **90**, 2384.
23 M. K. Nazeeruddin, A. Kay and M. Grätzel, *J. Am. Chem. Soc.*, 1993, **115**, 6382.
24 S. M. Yang, H. Z. Kou, S. L. Song, H. J. Wang and W. H. Fu, *Colloids Surf., A*, 2009, **340**, 182.
25 T. Z. Yu, W. M. Su, W. L. Li, Z. R. Hong, R. N. Hua, M. T. Li, B. Chu and B. Li, *Inorg. Chim. Acta*, 2006, **359**, 2246.
26 S. Ito, T. N. Murakami, P. Comte, P. Liska, C. Grätzel, M. K. Nazeeruddin and M. Grätzel, *Thin Solid Films*, 2008, **516**, 4613.
27 P. Wang, Z. Hong and Z. Xie, *Chem. Commun.*, 2003, 1664.
28 C. A. Mcaulliffe, A. C. Rice and W. E. Hill, *Inorg. Chim. Acta*, 1980, **45**, 115.
29 M. Asadi, K. A. Jamshid and A. H. Kyanfar, *Inorg. Chim. Acta*, 2007, **360**, 1725.
30 M. Tumer, H. Koksal, M. K. Sener and S. Serin, *Transition Met. Chem.*, 1999, **24**, 414.
31 G. A. Kohawole and K. S. J. Patel, *J. Chem. Soc., Dalton Trans.*, 1981, 1241.
32 F. A. Bottino, P. Finocchiaro and E. Libertini, *J. Coord. Chem.*, 1988, **16**, 341.
33 H. H. Freedman, *J. Am. Chem. Soc.*, 1961, **83**, 2900.
34 C. W Shi, S. Y. Dai, K. J. Wang, X. Pan, L. Y. Zeng, L. H. Hu, F. T. Kong and L. Guo, *Electrochim. Acta*, 2005, **50**, 2597.
35 B. F. Xue, Z. W. Fu, H. Li, X. Z. Liu, S. C. Cheng, J. Yao, D. M. Li, L. Q. Chen and Q. B. Meng, *J. Am. Chem. Soc.*, 2006, **128**, 8720.
36 Z. Zhang, S. M. Zakeeruddin, B. C. O'Regan, R. Humphry-Baker and M. Gratzel, *J. Phys. Chem. B*, 2005, **109**, 21818.